

## Interplay between spin-orbit coupling and ferromagnetism in magnetotransport properties of a spin-polarized oxide two-dimensional electron system

D. Stornaiuolo,<sup>1,2,\*</sup> B. Jouault,<sup>3</sup> E. Di Gennaro,<sup>1,2</sup> A. Sambri,<sup>1,2</sup> M. D'Antuono,<sup>1</sup> D. Massarotti,<sup>2,4</sup> F. Miletto Granozio,<sup>2</sup> R. Di Capua,<sup>1,2</sup> G. M. De Luca,<sup>1,2</sup> G. P. Pepe,<sup>1,2</sup> F. Tafuri,<sup>1,2</sup> and M. Salluzzo<sup>2</sup>

<sup>1</sup>*Dipartimento di Fisica Ettore Pancini, Università degli Studi di Napoli Federico II, Napoli, Italy*

<sup>2</sup>*CNR-SPIN, Complesso Monte Sant'Angelo via Cinthia, I-80126 Napoli, Italy*

<sup>3</sup>*Laboratoire Charles Coulomb, UMR 5221, CNRS, Université Montpellier 2, F-34095 Montpellier, France*

<sup>4</sup>*Dipartimento di Ingegneria Elettrica e Tecnologie dell'Informazione, Università degli Studi di Napoli Federico II, Napoli, Italy*



(Received 2 February 2018; revised manuscript received 9 May 2018; published 10 August 2018; corrected 26 November 2018)

We report on the magnetotransport properties of a spin-polarized two-dimensional electron system (2DES) formed in LaAlO<sub>3</sub> (LAO)/EuTiO<sub>3</sub>/SrTiO<sub>3</sub> (STO) heterostructures. We show that, at low temperature, the 2DES magnetoconductance exhibits weak antilocalization corrections related to Rashba spin-orbit scattering, in analogy with the LAO/STO 2DES. However, the characteristic spin-orbit scattering field decreases substantially for carrier density higher than  $1.9 \times 10^{13} \text{ cm}^{-2}$ . We attribute this behavior to the masking effect of ferromagnetism, which sets in at the same carrier density and at a temperature below 10 K. Our work shows that, while weak antilocalization corrections to the magnetoconductance are strongly reduced by the emergence of ferromagnetism, they persist in a large part of the phase diagram of a spin-polarized oxide 2DES.

DOI: [10.1103/PhysRevB.98.075409](https://doi.org/10.1103/PhysRevB.98.075409)

### I. INTRODUCTION

The exploitation of the large Rashba spin-orbit (SO) coupling in low-dimensional semiconducting systems is a viable route for electric field control of the spin transport in novel spintronic devices. In order to create a spin-polarized current, several approaches have been considered, such as spin injection into semiconductors using ferromagnets. However, the large conductivity mismatch and spin scattering at the interface limit the use of this method [1]. For this reason, scientists have investigated the possibility to combine the properties of semiconductors and ferromagnets in a single material, leading to the realization of diluted magnetic semiconductors, like ferromagnetic Mn-doped III-V semiconductors [2–4]. Electric field control of magnetic properties, a highly desirable feature for fundamental studies and technological applications, has been also demonstrated for these materials [5,6].

In recent years, interest on possible spintronic applications of the two-dimensional electron system (2DES) formed at the interface between LaAlO<sub>3</sub> and SrTiO<sub>3</sub> (LAO/STO) oxide insulators is emerging. The LAO/STO system shows a large and electric field tunable Rashba spin-orbit coupling [7,8], and an exceptionally large spin-to-charge conversion efficiency [9,10], comparable with what has been found in topological insulators. Moreover, recently a spin-polarized oxide 2DES has been designed and realized using a thin layer of delta doping EuTiO<sub>3</sub> (ETO) intercalated between LAO and STO [11]. X-ray magnetic circular dichroism and transport measurements performed on LAO/ETO/STO heterostructures indicate ferromagnetic properties with a characteristic temperature  $T_{\text{FM}} \approx 6\text{--}10$  K. Ferromagnetism in this heterostructure can

be tuned using electric field effect, giving the possibility to “switch” on and off the spin polarization in a continuous and reproducible way. In a wide range of carrier concentration for which the 2DES exhibits ferromagnetism in the normal state, moreover, superconductivity with a maximum  $T_c$  of 125 mK has also been found.

In the present work, we study the interplay between ferromagnetism and Rashba spin-orbit (SO) scattering in LAO/ETO/STO heterostructures by analyzing the quantum interference correction to the magnetoconductance data as a function of the carrier density and of the temperature.

In metals and semiconductors, quantum interference between time-reversed electron self-intersecting paths leads to an enhanced probability of backscattering which is called weak localization (WL). In the presence of sufficiently strong SO interaction, however, electrons traveling on time-reversed closed paths experience a spin rotation in opposite directions, which causes a destructive interference of the two partial electron waves and reduced backscattering, leading to weak antilocalization (WAL). An applied magnetic field reduces the carriers' phase coherence length and washes out quantum interference, suppressing both WL and WAL. Therefore, WL and WAL corrections to the conductivity manifest as a negative (in the case of WL) or positive (in the case of WAL) magnetoresistance (MR) effect.

In ferromagnets, the observation of WL or WAL is more complex due to the presence of competing factors, such as the anisotropic magnetoresistance (AMR) effect and internal magnetic fields, which can either destroy quantum interference or mask its occurrence [12–14]. For instance, in the case of (GaAs)Mn, contrary to common ferromagnetic materials, the resistivity is larger when the magnetization is perpendicular to the current, compared to the case when the magnetization is parallel to the current. For in-plane spontaneous magnetization,

\*stornaiuolo@fisica.unina.it

this corresponds to a maximum of conductivity at zero field followed by a minimum and eventually an increase up to the saturation field, resulting in a strong AMR peak [13]. In clean, strong ferromagnets, where the magnetic scattering length  $L_M$  is smaller than the mean free path and of the SO scattering length, neither WL nor WAL survive. On the other hand, weak and disordered ferromagnets can show quantum interference effects, as demonstrated in (Ga,Mn)As nanodevices by measurements of universal conductance fluctuations and Aharonov-Bohm effects [15,16]. However, conflicting conclusions have been reached on the magnitude and even on the sign of quantum corrections to the conductivity in this system.

The recent realization of a tunable, spin-polarized oxide 2DES offers a new system for the test of these complex interactions. We show that the magnetoconductance quantum corrections associated to SO scattering are deeply influenced by the emergence of a ferromagnetic coupling, which, in this system, can be tuned both by carrier concentration and by temperature. On the other hand, WAL corrections are still observed in this 2DES deep in the ferromagnetic phase.

## II. SAMPLES FABRICATION AND GENERAL PROPERTIES

LAO (10 u.c.)/ETO (2 u.c.) heterostructures are realized by reflection high-energy electron diffraction-assisted pulsed laser deposition onto TiO<sub>2</sub>-terminated (001) STO substrates [Fig. 1(a)]. A KrF excimer laser (wavelength, 248 nm; pulse rate, 1 Hz) is focused on sintered Eu<sub>2</sub>Ti<sub>2</sub>O<sub>7</sub> and crystalline

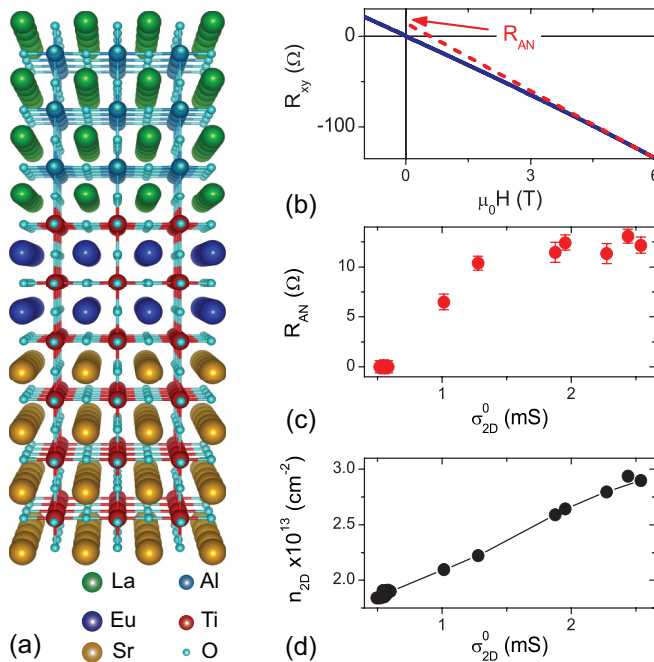


FIG. 1. (a) Crystal structure of LAO/ETO/STO heterostructures. (b) Transverse resistance  $R_{xy}$  measured at  $n_{2D} = 2.9 \times 10^{13} \text{ cm}^{-2}$ . The zero field extrapolation of the linear part of the curve defines the anomalous component  $R_{AN}$ . (c) Evolution of  $R_{AN}$  with the sheet conductance, tuned by electric field effect. (d) 2D number of carriers (measured using Hall effect) as a function of the sheet conductance.

LAO targets at a fluence of  $1.3 \text{ J/cm}^2$ . During the deposition, the samples are kept at  $680^\circ \text{C}$  in oxygen partial pressure  $p[\text{O}_2]$  of  $1 \times 10^{-4} \text{ mbar}$ . Following deposition, the samples are slowly cooled down to room temperature at a rate of  $3^\circ \text{C/min}$ , in  $p[\text{O}_2] = 1 \times 10^{-4} \text{ mbar}$  [17].

The LAO/ETO/STO system shows an orbital reconstruction similar to that of LAO/STO 2DES [18,19] and an inversion of the bands compared to bulk STO [11,17]. In the present work, we performed magnetotransport measurements on LAO/ETO/STO samples using van der Pauw configuration down to  $T = 1.8 \text{ K}$  and in magnetic field up to 9 T. The carrier concentration was tuned by electric field effect in the back gate configuration. The measurements were realized by injecting drive currents between 100 and 400 nA, and reading the samples voltage response using low-noise amplification stages and lock-in amplifiers.

Panel (b) of Fig. 1 shows transverse resistance  $R_{xy}$  measurements performed at high carrier concentration ( $n_{2D} = 2.9 \times 10^{13} \text{ cm}^{-2}$ ). The data exhibit a downward curvature at  $H \approx 2 \text{ T}$ , which is a manifestation of anomalous Hall effect appearing for carrier densities above  $n_c = 1.9 \times 10^{13} \text{ cm}^{-2}$  [corresponding to a sheet conductance  $\sigma_c$  of  $0.7 \text{ mS}$ ; see panel (d)], and is perfectly correlated to the magnetization of the system [11]. Thus, the 2DES becomes spin polarized at  $\sigma_{2D}^0 > \sigma_c$ , as shown in Fig. 1(c), where we plot the anomalous resistance  $R_{AN}$  (defined as the zero field extrapolation of the  $R_{xy}$  linear part, between 4 and 6 T) as a function of the electric field tuned sheet conductance.

## III. MAGNETORESISTANCE DATA AND FIT

Figure 2(a) shows selected differential MR curves acquired applying the external magnetic field perpendicular to the interface, for several values of the gate-tuned sheet conductance  $\sigma_{2D}^0$ . The data were symmetrized in order to remove any possible Hall component. For all the carrier concentration levels studied, besides the classical parabolic magnetoresistance term [20], we observe a positive MR at low field, which persists when the applied magnetic field is in the plane of the 2DES, as shown in Fig. 2(b).

A similar positive low field curvature of the MR data is observed in the case of the STO and LAO/STO 2DES, and it is attributed to the WAL correction associated to the SO interaction. On the other hand, in the case of ferromagnetic LAO/ETO/STO, the AMR effect could contribute to the magnetoresistance, masking the quantum corrections related to weak antilocalization.

In order to estimate the magnitude of the AMR contribution in our data, we performed measurements of the longitudinal resistance  $R$  in different configurations, both with magnetic field applied perpendicular to the current ( $R_z$  and  $R_y$ ) and parallel to the current ( $R_x$ ) [21] (see sketch in Fig. 3). In Fig. 3(a) the AMR, defined as  $(R_x - R_y)/R_x(0)$  (in-plane AMR) and  $(R_x - R_z)/R_x(0)$  (out-of-plane AMR) is shown for  $\sigma_{2D}^0 = 2.4 \text{ mS}$  (corresponding to  $n_{2D} = 2.9 \times 10^{13} \text{ cm}^{-2}$ ), deep in the ferromagnetic (FM) phase. One can see that the out-of-plane AMR is almost flat between  $-2$  and  $2 \text{ Tesla}$  (and close to zero), and the in-plane AMR has a parabolic shape without a change in the curvature in a large magnetic field range. This shows that below 2 T, the FM magnetization orientation

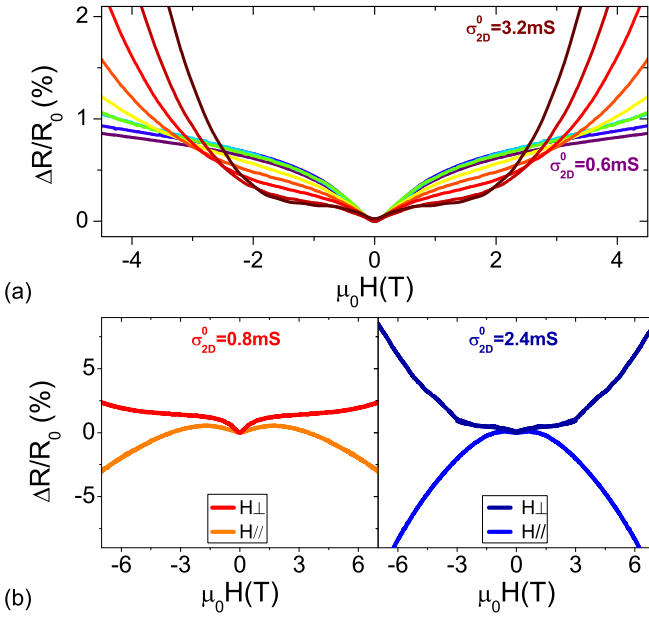


FIG. 2. (a) Differential MR curves of LAO/ETO/STO heterostructure as a function of gate voltage measured at  $T = 1.9$  K applying the magnetic field perpendicular to the 2DES plane. Panel (b) shows MR curves measured at  $n_{2D} = 2 \times 10^{13} \text{ cm}^{-2}$  (left panel) and  $n_{2D} = 3 \times 10^{13} \text{ cm}^{-2}$  (right panel) applying the magnetic field both perpendicular and parallel to the 2DES plane.

with the field cannot explain the magnetoconductance peak observed in both parallel and perpendicular magnetic field.

Therefore, we attribute the low field curvature of our MR data to WAL correction associated to SO interaction, similarly to the case of LAO/STO 2DES [7].

In order to study the evolution of the SO coupling as a function of the field-effect modulated carrier concentration,

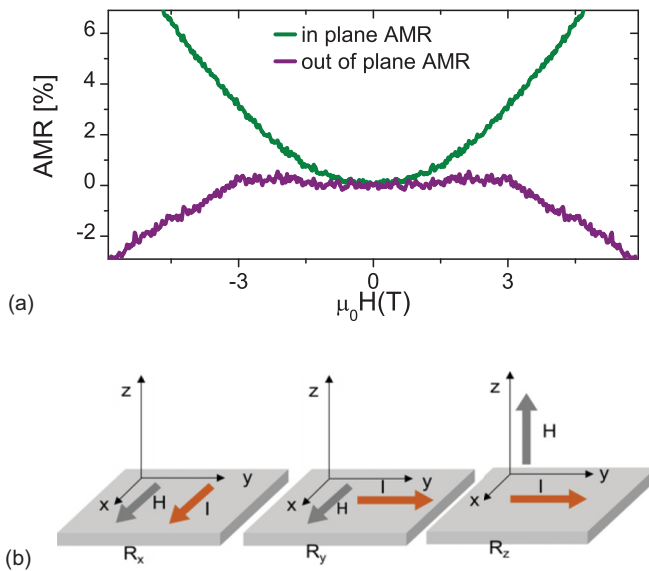


FIG. 3. (a) In-plane (green) and out-of-plane (purple) AMR in the FM phase of LAO/ETO/STO measured at  $T = 1.8$  K and  $\sigma_{2D}^0 = 2.4$  mS. (b) Sketch of the measurement configurations. The 2DES is in the  $x$ - $y$  plane.

we analyze the magnetoconductance (MC) curves to extract the characteristic transport parameters. Since a theoretical model for a 2DES characterized by a strong Rashba SO coupling, weak magnetism, and intermediate disorder has not been developed yet, we resort to nonmagnetic models. The limits emerging from this choice will be discussed later. The two most widely used WL/WAL theoretical models were developed by Hikami, Larkin, and Nagaoka (HLN) [22] and by Iordanskii, Lyanda-Geller, and Pikus (ILP) [23]. The former is based on the Elliott-Yafet spin-flip scattering mechanism and incorporates only the  $k$ -cubic SO coupling term, whereas the latter is based on the Dyakonov-Perel spin precession mechanism and takes into account both the  $k$ -linear and  $k$ -cubic SO coupling (where  $k$  is the wave vector of the carrier). The Rashba SO coupling in oxide 2DES originates from the Dyakonov-Perel mechanism [7], therefore in this work we use the ILP formalism. As shown in the Supplemental Material, optimal fitting of experimental data can be obtained neglecting the  $k$ -linear term in the ILP formula. In this case, the formula acquires the following closed form:

$$\begin{aligned} \frac{\Delta\sigma(B)}{\sigma_0} = & \psi\left(\frac{1}{2} + \frac{B_\phi}{B} + \frac{B_{so}}{B}\right) \\ & + \frac{1}{2}\psi\left(\frac{1}{2} + \frac{B_\phi}{B} + 2\frac{B_{so}}{B}\right) - \frac{1}{2}\psi\left(\frac{1}{2} + \frac{B_\phi}{B}\right) \\ & - \ln\frac{B_\phi + B_{so}}{B} - \frac{1}{2}\ln\frac{B_\phi + 2B_{so}}{B} + \frac{1}{2}\ln\frac{B_\phi}{B} \\ & - A_k \frac{\sigma_{2D}^0}{\sigma_0} \frac{(\mu B)^2}{1 + A_k(\mu B)^2}, \end{aligned} \quad (1)$$

where  $\Delta\sigma(B) = \sigma_{2D}(B) - \sigma_{2D}^0$  (with  $\sigma_{2D}^0$  the sheet conductance at zero magnetic field),  $\psi(x)$  is the digamma function,  $\sigma_0 = e^2/\pi h$ , and  $B_\phi$  and  $B_{so}$  are the characteristic magnetic fields for the phase coherence and the SO coupling, respectively. The last term of Eq. (1), involving the parameter  $A_k$ , gives an account of the classical parabolic MC. We point out that, for LAO/STO, the Maekawa and Fukuyama (MF) formula [24], a development of the HLN theory, has been often used with good results. This success is due to the mathematical identity of the models when only the  $k$ -cubic term is taken into account [25].

Figure 4(a) shows the experimental differential MC curves and the fit performed using Eq. (1) (black lines). The SO field values  $B_{so}$  obtained from the fit are reported in Figure 4(b). In the same plot we show also data from LAO/STO heterostructures, adapted from Ref. [26]. In order to perform this comparison, the fit parameters in this figure are plotted versus the field-effect modulated sheet conductance  $\sigma_{2D}^0$ , which is directly related to the carrier concentration. At low conductance (carrier concentration), the SO coupling field of LAO/ETO/STO follows that of the LAO/STO 2DES, having roughly the same values and the same increasing behavior with the carrier concentration. Above  $\sigma_{2D}^0 \approx 0.7$  mS, however, the behavior changes abruptly, and the SO coupling field of LAO/ETO/STO starts to decrease with the carrier concentration. We point out that this behavior was found in several samples and using both the ILP and the MF theory [inset of Fig. 4(b)]. Interestingly, the change in slope of  $B_{so}$  vs  $\sigma_{2D}^0$

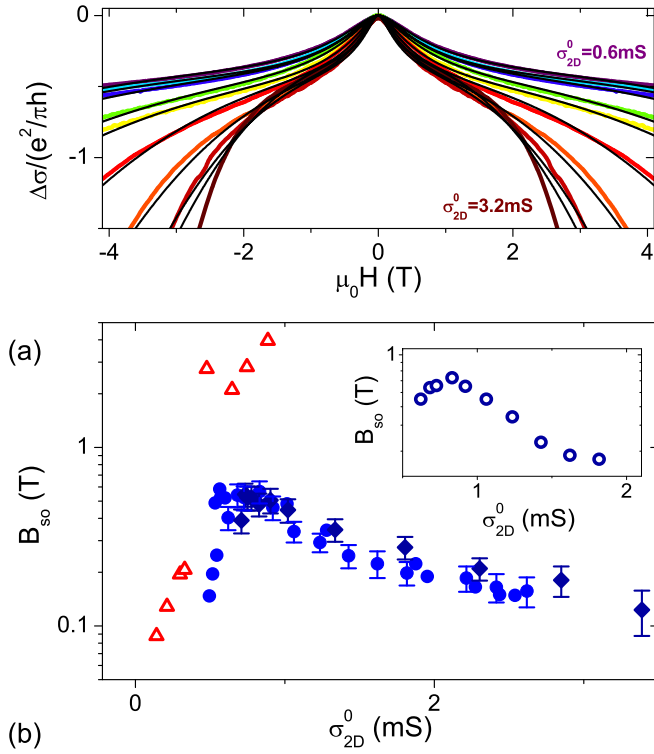


FIG. 4. (a) Differential magnetoconductance data  $\Delta\sigma_{2D} = \sigma_{2D}(H) - \sigma_{2D}^0$  plot in units of  $\sigma_0 = e^2/\pi h$  measured at  $T = 1.9$  K on LAO/ETO/STO. The full black lines are the fit using Eq. (1). (b) Spin-orbit field  $B_{so}$  obtained from the fit. The blue circles and diamonds refer to two LAO/ETO/STO samples, whereas the red triangles are data for LAO/STO adapted from Ref. [26]. The procedure used to evaluate the error bars on the fit parameters is reported in the Supplemental Material. For some of the data points, the error bars are smaller than the size of the symbol used, thus not visible. In the inset, the  $B_{so}$  obtained fitting the same curves with the MF formula is reported.

takes place at a sheet conductance value very close to that found for the activation of ferromagnetic effects [Fig. 2(c)] [11].

In order to disentangle the magnetic and SO coupling information encoded in the MC curves, we measured the Hall effect and the magnetoconductance of LAO/ETO/STO samples as a function of the temperature. Panel (a) of Fig. 5 shows the temperature behavior of the anomalous component of the Hall effect  $R_{AN}$  measured for values of  $\sigma_{2D}^0$  between 0.6 and 2.4 mS (corresponding to  $n_{2D}$  between  $2.0$  and  $2.8 \times 10^{13} \text{ cm}^{-2}$ ). As shown in Ref. [11],  $R_{AN}$  vanishes at a ferromagnetic critical temperature  $T_{FM}$  consistent with x-ray magnetic circular dichroism (XMCD) measurements. Interestingly,  $T_{FM}$  changes with field-effect modulated carrier concentration: at high carrier concentration ( $\sigma_{2D}^0 = 2.4$  mS) ferromagnetic effects are robust and well visible in the Hall effect up to  $T_{FM} \approx 10$  K, whereas at  $\sigma_{2D}^0 = 0.8$  mS,  $T_{FM}$  is reduced to 6 K.

Figure 5(b) shows the values of  $B_\phi$  and  $B_{so}$  extracted from the fit of the MC curves measured at various temperatures for two values of the sheet conductance. Instead of showing the expected temperature-independent behavior [20,26,27],  $B_{so}$  clearly increases with increasing temperature, mimicking the

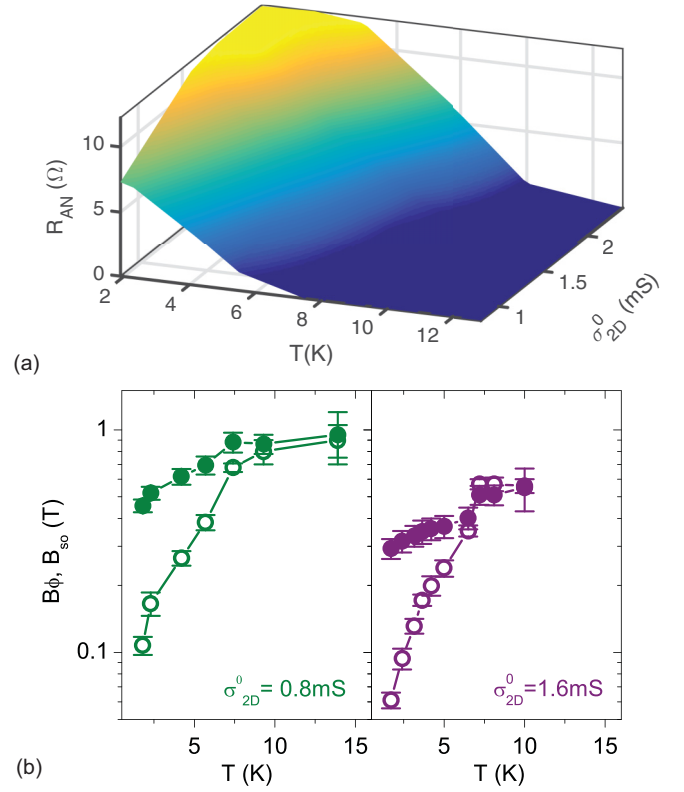


FIG. 5. (a) Temperature behavior of the anomalous Hall effect component  $R_{AN}$  [defined in Fig. 1(c)] as a function of the sheet conductance. (b) Temperature behavior of  $B_\phi$  (open symbols) and  $B_{so}$  (filled symbols) for  $\sigma_{2D}^0 = 0.8$  mS (left panel) and 1.6 mS (right panel). The error bars were estimated following the procedure described in the Supplemental Material.

concomitant reduction of  $R_{AN}$  and of the magnetization. At 6 and 7.5 K,  $B_{so}$  reaches maximum values which are twice those obtained at low  $T$  [28]. These temperatures are in good agreement with the  $T_{FM}$  shown in panel (a) for  $\sigma_{2D}^0 = 0.8$  and 1.6 mS, respectively.

#### IV. DISCUSSION AND CONCLUSIONS

All the data available on LAO/STO 2DES report a monotonic increasing behavior of  $B_{so}$  (corresponding to monotonic decrease of SO scattering time  $\tau_{so}$ ) as a function of the carrier concentration [7,26,29], with the only exception of Ref. [30], where the authors observe a nonmonotonic behavior ascribed to a single- to two-carrier transition in correspondence of the Fermi level crossing of different  $d$  bands. In our case, as mentioned above, we ascribe the apparent reduction of  $B_{so}$  for  $n_{2D} > 2.0 \times 10^{13} \text{ cm}^{-2}$  to the emergence of FM, which reduces the WAL corrections to the magnetoconductance, but does not suppress them completely. While FM in LAO/ETO/STO takes place at a doping close to the Lifshitz point, at which the density of  $3d_{xz,yz}$  carriers have a steep increase [11], the temperature dependence of  $B_{so}$  shown in this work cannot be explained without invoking the role of magnetic correlations in the 2DES. Figure 5 indeed demonstrates that the SO field obtained from the magnetoconductance curves fit increases with the

temperature as a result of the reduction in magnetization approaching  $T_{\text{FM}}$ . Moreover, the temperature increase of  $B_{\text{so}}$  is steeper at low carrier concentration (low  $\sigma_{2\text{D}}^0$ ), where FM disappears around 6 K, compared to high carrier concentration data (high  $\sigma_{2\text{D}}^0$ ).

Interestingly, our data clearly show that WAL in LAO/ETO/STO magnetoconductance does not disappear even at the highest carrier density. This behavior differs from that of conventional thin metallic ferromagnetic films. According to the theory, the quantum corrections to the conductivity of a ferromagnetic system are suppressed when the magnetic scattering length  $L_M = (D\hbar/M)^{1/2}$  (where  $D$  is the diffusion constant and  $M$  is the magnetic exchange coupling constant) [31] associated to the ferromagnetic order or to the presence of magnetic impurities, is smaller than the inelastic or than the spin-orbit scattering length  $L_{\text{so}}$  (with  $B_{\text{so}} = \hbar/4eL_{\text{so}}^2$ ). We point out that, due to the absence of a theoretical magnetoconductance model suitable for the intermediate regime of spin-orbit coupling and magnetic splitting which applies to our system, we fit our MC data using nonmagnetic models. Thus, while the reduction of the  $B_{\text{so}}$  values in the ferromagnetic phase is a direct indication that the spin-orbit scattering induced WAL contribution is suppressed, the same values cannot be directly correlated to the SO scattering length and times. For this reason, we evaluate  $L_{\text{so}}$  just before the 2DES enters the ferromagnetic phase and we find  $L_{\text{so}} = 36$  nm. As a consequence, the WAL correction should survive only if  $L_M > 36$  nm, corresponding to a magnetic exchange  $M < 1$  meV. This value of  $M$  is much lower than that of conventional ferromagnetic films and of dilute GaAsMn semiconductors [32]. We point out, however, that in Ref. [11] a magnetic exchange parameter of the order of 10 meV was extracted from the fit of the Ti-edge XMCD data (at high field) of LAO/ETO/STO. On qualitative grounds, we propose that the

results can be in part reconciled by considering both the kind of magnetic order and the magnetization orientation in LAO/ETO/STO. The magnetization easy axis in (001) LAO/ETO/STO is parallel to the interface, therefore it does not affect electron orbits. Increasing the magnetic field, however, the out-of-plane magnetization increases and reaches values comparable to the in-plane magnetization at about 3–4 T [11]. Thus, at low field, quantum corrections to the conductivity are not fully suppressed, while at higher field other effects should be considered, including anisotropic magnetoresistance and possibly electron-electron interaction contributions.

In summary, we have shown that quantum interference effects strongly influences the low-temperature conductance of spin-polarized LAO/ETO/STO 2DES, which show WAL also at highest carrier density, at which the ferromagnetic correlation reaches maximum values. Thanks to the low  $T_{\text{FM}}$  of our system, we were able to investigate the competition between Rashba SO coupling and FM induced corrections also as a function of the temperature. We show that ferromagnetism masks, but does not wipe out, WAL corrections. The latter indeed reemerge when ferromagnetic correlations are reduced approaching  $T_{\text{FM}}$ . These results suggest that the LAO/ETO/STO spin-polarized 2DES, characterized by large and tunable Rashba SOC and magnetism, is a possible candidate for quantum spintronic applications.

#### ACKNOWLEDGMENTS

The authors thank S. Gariglio and J.-M. Triscone for useful discussions. This work was partially supported by COST Action CA16218 and by the project Quantox of QuantERA ERA-NET Cofund in Quantum Technologies (Grant Agreement No. 731473) implemented within the European Union's Horizon 2020 Programme.

- 
- [1] P. R. Hammar, B. R. Bennett, M. J. Yang, and M. Johnson, *Phys. Rev. Lett.* **83**, 203 (1999).
  - [2] H. Ohno, H. Munekata, T. Penney, S. von Molnar, and L. L. Chang, *Phys. Rev. Lett.* **68**, 2664 (1992).
  - [3] H. Ohno, A. Shen, F. Matsukura, A. Oiwa, A. Endo, S. Katsumoto, and Y. Iye, *Appl. Phys. Lett.* **69**, 363 (1996).
  - [4] T. Jungwirth, J. Wunderlich, V. Novák, K. Olejnik, B. Gallagher, R. Campion, K. Edmonds, A. Rushforth, A. Ferguson, and P. Němec, *Rev. Mod. Phys.* **86**, 855 (2014).
  - [5] H. Ohno, D. Chiba, F. Matsukura, T. Omiya, E. Abe, T. Dietl, Y. Ohno, and K. Ohtani, *Nature (London)* **408**, 944 (2000).
  - [6] D. Chiba, F. Matsukura, and H. Ohno, *Appl. Phys. Lett.* **89**, 162505 (2006).
  - [7] A. D. Caviglia, M. Gabay, S. Gariglio, N. Reyren, C. Cancellieri, and J.-M. Triscone, *Phys. Rev. Lett.* **104**, 126803 (2010).
  - [8] M. Ben Shalom, M. Sachs, D. Rakhmilevitch, A. Palevski, and Y. Dagan, *Phys. Rev. Lett.* **104**, 126802 (2010).
  - [9] E. Lesne, Y. Fu, S. Oyarzun, J. C. Rojas-Sánchez, D. C. Vaz, H. Naganuma, G. Sicoli, J.-P. Attané, M. Jamet, E. Jacquet *et al.*, *Nat. Mater.* **15**, 1261 (2016).
  - [10] J.-Y. Chaudreau, M. Boselli, S. Gariglio, R. Weil, G. De Loubens, J.-M. Triscone, and M. Viret, *Europhys. Lett.* **116**, 17006 (2016).
  - [11] D. Stornaiuolo, C. Cantoni, G. De Luca, R. Di Capua, E. DiGennaro, G. Ghiringhelli, B. Jouault, D. Marrè, D. Massarotti, F. Miletto-Granozio *et al.*, *Nat. Mater.* **15**, 278 (2016).
  - [12] V. K. Dugaev, P. Bruno, and J. Barnaś, *Phys. Rev. B* **64**, 144423 (2001).
  - [13] D. Neumaier, K. Wagner, S. Geißler, U. Wurstbauer, J. Sadowski, W. Wegscheider, and D. Weiss, *Phys. Rev. Lett.* **99**, 116803 (2007).
  - [14] I. Garate, J. Sinova, T. Jungwirth, and A. H. MacDonald, *Phys. Rev. B* **79**, 155207 (2009).
  - [15] K. Wagner, D. Neumaier, M. Reinwald, W. Wegscheider, and D. Weiss, *Phys. Rev. Lett.* **97**, 056803 (2006).
  - [16] L. Vila, R. Giraud, L. Thevenard, A. Lemaitre, F. Pierre, J. Dufouleur, D. Mailly, B. Barbara, and G. Faini, *Phys. Rev. Lett.* **98**, 027204 (2007).
  - [17] G. De Luca, R. Di Capua, E. Di Gennaro, F. Miletto-Granozio, D. Stornaiuolo, M. Salluzzo, A. Gadaleta, I. Pallecchi, D. Marrè, C. Piamonteze *et al.*, *Phys. Rev. B* **89**, 224413 (2014).
  - [18] M. Salluzzo, J. Cezar, N. Brookes, V. Bisogni, G. De Luca, C. Richter, S. Thiel, J. Mannhart, M. Huijben, A. Brinkman *et al.*, *Phys. Rev. Lett.* **102**, 166804 (2009).

- [19] P. Delugas, A. Filippetti, V. Fiorentini, D. I. Bilc, D. Fontaine, and P. Ghosez, *Phys. Rev. Lett.* **106**, 166807 (2011).
- [20] See Supplemental Material at <http://link.aps.org/supplemental/10.1103/PhysRevB.98.075409> for more details on the fit of the magnetoconductance curves using the ILP formula, on the evaluation of the orbital contribution to the magnetoconductance data and on the temperature behavior of the magnetoconductance curves.
- [21] D. V. Baxter, D. Ruzmetov, J. Scherschligt, Y. Sasaki, X. Liu, J. K. Furdyna, and C. H. Mielke, *Phys. Rev. B* **65**, 212407 (2002).
- [22] S. Hikami, A. I. Larkin, and Y. Nagaoka, *Prog. Theor. Phys.* **63**, 707 (1980).
- [23] S. Iordanskii, Y. B. Lyanda-Geller, and G. Pikus, *Zh. Eksp. Teor. Fiz., Pis'ma Red.* **60**, 199 (1994).
- [24] S. Maekawa and H. Fukuyama, *J. Phys. Soc. Jpn.* **50**, 2516 (1981).
- [25] The approach we follow remains valid also in the presence of a complex Fermi surface with multiple bands. In this case, the parameters extracted from the fittings cannot in general be representative of the physical characteristics of each band separately, but should be considered as effective (average) values [33].
- [26] D. Stornaiuolo, S. Gariglio, A. Fête, M. Gabay, D. Li, D. Massarotti, and J.-M. Triscone, *Phys. Rev. B* **90**, 235426 (2014).
- [27] G. Bergmann, *Phys. Rev. Lett.* **48**, 1046 (1982).
- [28] A similar increase in  $B_{so}$  is seen also for higher values of  $\sigma_{2D}^0$ . However, in this case, the estimation of the scattering fields at high temperature is less reliable due to the larger contribution of the classical parabolic term.
- [29] G. Herranz, G. Singh, N. Bergeal, A. Jouan, J. Lesueur, J. Gázquez, M. Varela, M. Scigaj, N. Dix, F. Sánchez, and J. Fontcuberta, *Nat. Commun.* **6**, 6028 (2015).
- [30] H. Liang, L. Cheng, L. Wei, Z. Luo, G. Yu, C. Zeng, and Z. Zhang, *Phys. Rev. B* **92**, 075309 (2015).
- [31] V. K. Dugaev, P. Bruno, and J. Barnaś, *Phys. Rev. Lett.* **101**, 129701 (2008).
- [32] T. Dietl, H. Ohno, and F. Matsukura, *Phys. Rev. B* **63**, 195205 (2001).
- [33] D. Rainer and G. Bergmann, *Phys. Rev. B* **32**, 3522 (1985).

*Correction:* A misspelling in the fourth affiliation has been corrected.